*Inorg. Chem.* **2005**, *44*, 3561–3568


# Separation and Characterization of the Two Diastereomers for $[Gd(DTPA\text{-}bz\text{-}NH_2)(H_2O)]^{2-}$, a Common Synthon in Macromolecular MRI Contrast Agents: Their Water Exchange and Isomerization Kinetics

**László Burai,† Éva Tóth,* Angélique Sour,† and André E. Merbach†**

*Laboratoire de Chimie Inorganique et Bioinorganique, Ecole Polytechnique Fédérale de Lausanne, EPFL-BCH, CH-1015 Lausanne, Switzerland*

Received September 27, 2004

Chiral, bifunctional poly(amino carboxylate) ligands are commonly used for the synthesis of macromolecular, $Gd^{III}$-based MRI contrast agents, prepared in the objective of increasing relaxivity or delivering the paramagnetic $Gd^{III}$ to a specific site (targeting). Complex formation with such ligands results in two diastereomeric forms for the complex which can be separated by HPLC. We demonstrated that the diastereomer ratio for $Ln^{III}$ DTPA derivatives (~60:40) remains constant throughout the lanthanide series, in contrast to $Ln^{III}$ EPTPA derivatives, where it varies as a function of the cation size with a maximum for the middle lanthanides ($DTPA^{5-}$ = diethylenetriaminepentaacetate; $EPTPA^{5-}$ = ethylenepropylenetriaminepentaacetate). The interconversion of the two diastereomers, studied by HPLC, is a proton-catalyzed process ($k_{obs} = k_1[H^+]$). It is relatively fast for $[Gd(EPTPA\text{-}bz\text{-}NH_2)(H_2O)]^{2-}$ but slow enough for $[Gd(DTPA\text{-}bz\text{-}NH_2)(H_2O)]^{2-}$ to allow investigation of pure individual isomers (isomerization rate constants are $k_1 = (3.03 \pm 0.07) \times 10^4$ and $11.6 \pm 0.5$ $s^{-1}$ $M^{-1}$ for $[Gd(EPTPA\text{-}bz\text{-}NH_2)(H_2O)]^{2-}$ and $[Gd(DTPA\text{-}bz\text{-}NH_2)(H_2O)]^{2-}$, respectively). Individual water exchange rates have been determined for both diastereomers of $[Gd(DTPA\text{-}bz\text{-}NH_2)(H_2O)]^{2-}$ by a variable-temperature $^{17}O$ NMR study. Similarly to $Ln^{III}$ EPTPA derivatives, $k_{ex}$ values differ by a factor of 2 ($k_{ex}^{298} = (5.7 \pm 0.2) \times 10^6$ and $(3.1 \pm 0.1) \times 10^6$ $s^{-1}$). This variance in the exchange rate has no consequence on the proton relaxivity of the two diastereomers, since it is solely limited by fast rotation. However, such difference in $k_{ex}$ will affect proton relaxivity when these diastereomers are linked to a slowly rotating macromolecule. Once the rotation is optimized, slow water exchange will limit relaxivity; thus, a factor of 2 in the exchange rate can lead to a remarkably different relaxivity for the diastereomer complexes. These results have implications for future development of $Gd^{III}$-based, macromolecular MRI contrast agents, since the use of chiral bifunctional ligands in their synthesis inevitably generates diastereomeric complexes.

## Introduction

During the past decades, metal complexes have acquired an important role in medical diagnosis and therapy. Complexes of $\gamma$-emitting metal ions such as $^{99m}Tc$, $^{111}In$, or $^{67}Ga$ are useful tools for obtaining diagnostic information,[1] while those of particle-emitting isotopes such as the $\beta$-emitter $^{90}Y$ or $^{186}Re$ can be used in internal radiotherapy.[2] Paramagnetic $Gd^{III}$ complexes are extensively applied as contrast enhancing agents in magnetic resonance imaging (MRI).[3] In medical applications involving metal chelates, $DTPA^{5-}$ is one of the most commonly used ligands. This is mainly explained by the remarkable thermodynamic stability of the DTPA complexes, one of the highest among linear chelates. $[Gd(DTPA)(H_2O)]^{2-}$ was the first MRI contrast agent approved for clinical application (1988) and probably still remains the most widespread.

The attachment of a "reactive" pending arm to DTPA or other small ligands leads to bifunctional agents and allows

* Author to whom correspondence should be addressed. E-mail: eva.jakabtoth@epfl.ch. Tel: +41 21 693 9878. Fax: +41 21 693 9875.
† E-mail: laszlo.burai@epfl.ch (L.B.); angelique.sour@epfl.ch (A.S.); andre.merbach@epfl.ch (A.E.M.).

(1) (a) Schwochau, K. *Angew. Chem., Int. Ed. Engl.* **1994**, *33*, 2258. (b) McMurry, T. C.; Brechbiel, M.; Wu, C.; Gansow, O. A. *Bioconjugate Chem.* **1993**, *4*, 236. (c) Craig, A. S.; Parker, D.; Adams, H.; Bailey, N. A. *J. Chem. Soc., Chem. Commun.* **1989**, 1793.

(2) (a) Moi, A. K.; Meares, C. F.; DeNardo, S. J. *J. Am. Chem. Soc.* **1988**, *110*, 6266. (b) Heppeler, A.; Froidevaux, S.; Mäcke, H. R.; Jermann, E.; Béhé, M.; Powell, P.; Hennig, M. *Chem.—Eur. J.* **1999**, *5*, 1974.

(3) Tóth, É.; Helm, L.; Merbach, A. E. Relaxivity of Gadolinium(III) Complexes: Theory and Mechanism. In *The Chemistry of Contrast Agents in Medical Magnetic Resonance Imaging*; Tóth, É., Merbach, A. E., Eds.; Wiley: Chichester, U.K., 2001; pp 45−120.

10.1021/ic048645d CCC: $30.25 
Published on Web 04/15/2005

**Chart 1**

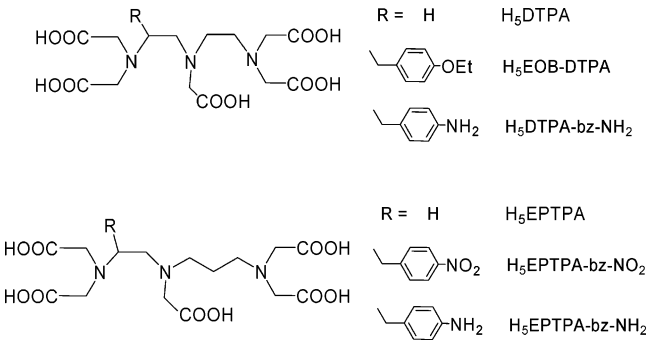


covalent binding to macromolecules.[4] Macromolecules such as monoclonal antibodies carrying one or several complexes can vehicle e.g. the radioactive metal to a specific tissue in selective cancer therapy. In MRI, large molecules loaded with $Gd^{III}$ have an improved efficiency due to their increased size, or they can also allow for targeted imaging.[5]

The isothiocyanato functional group is a very common linker for attaching small ligands such as DTPA to macromolecules. In the coupling reaction, the *p*-aminobenzyl derivative of the ligand is the starting compound. The $-NH_2$ of the *p*-aminobenzyl pending arm is transformed to an isothiocyanato function prior to the reaction with the macromolecule. These bifunctional, *p*-aminobenzyl derivatives are commercially available for a variety of ligands, and they are indeed widely used in the synthesis of macromolecules for biomedical applications. The presence of the *p*-aminobenzyl (or other) pending group in the 4-position of DTPA (Chart 1) generates a chiral center. On coordination of the central nitrogen (6-position) to the metal ion, a second chiral center arises which leads to two diastereomers (4*S*6*S*, 4*R*6*R* and 4*S*6*R*, 4*R*6*S*). Diastereomers may have different physicochemical properties and can be separated by chromatographic methods. HPLC separation has been performed in the case of some Ln(DTPA) derivatives. For $[Y(DTPA\text{-}bz\text{-}NH_2)(H_2O)]^{2-}$, Cummins et al. reported a 60:40 diastereomeric ratio as determined by HPLC.[6] Similar values (63:37) were found by NMR spectroscopy as well. A detailed HPLC study was reported for the $Gd^{3+}$ complex of another chiral DTPA derivative, $[Gd(S\text{-EOB-DTPA})(H_2O)]^{2-}$, which is a new liver-specific MRI contrast agent (Primovist, Schering AG).[7] Interestingly, the diastereomeric ratio was very similar, 65:35. After preparative HPLC separation of the $[Gd(S\text{-EOB-DTPA})(H_2O)]^{2-}$ diastereomers, the kinetics of their interconversion was also studied. Under physiological conditions it is very slow; several days are needed to return to equilibrium.

With regard to MRI contrast agent application, the water exchange rate of the $Gd^{III}$ complex is one of the crucial parameters to influence relaxivity, thus efficiency of the agent. Diastereomers having different structure can exhibit different water exchange rate. So far, no data are known for the water exchange of individual isomers of chiral $[Gd(DTPA)(H_2O)]^{2-}$ derivatives. Recently in a preliminary communication on $[Ln(EPTPA\text{-}bz\text{-}NH_2)(H_2O)]^{2-}$ and $[Ln(EPTPA\text{-}bz\text{-}NO_2)(H_2O)]^{2-}$ diastereomers, we have reported that the diastereomeric ratio (93:7) is independent of the pending arm, whereas it remarkably changes along the lanthanide series (Chart 1).[8] For the first time, we have determined the individual water exchange rates for the two diastereomers of these complexes. In the case of both $[Ln(EPTPA\text{-}bz\text{-}NH_2)(H_2O)]^{2-}$ and $[Ln(EPTPA\text{-}bz\text{-}NO_2)(H_2O)]^{2-}$, the water exchange was found to be twice as fast for the minor than for the major isomer. The Gd(EPTPA) derivatives can be regarded as potential building blocks for macromolecular MRI contrast agents, since their water exchange is faster thus closer to optimal than that for typical commercial $Gd^{III}$ complexes.[9] The water exchange rate plays a much more important role for slowly rotating macromolecular complexes than for small chelates, as the relaxivity of macromolecules can be largely limited by slow exchange, whereas, for small complexes, it is (almost) exclusively fast rotation that limits relaxivity. For the development of highly efficient macromolecular contrast agents one should be able to fine-tune the water exchange rate so that it falls into an optimal and relatively restricted range. Consequently, differences such as that found for the $[Gd(EPTPA\text{-}bz\text{-}NH_2)(H_2O)]^{2-}$ and $[Gd(EPTPA\text{-}bz\text{-}NO_2)(H_2O)]^{2-}$ diastereomers can be of great importance. The diastereomer with a more optimal water exchange rate bound to a macromolecule will exhibit higher relaxivity, provided the isomerization rate is slow enough to avoid the interconversion of the isomer during the time of a medical MRI investigation.

The objective of this study was 2-fold: (i) to establish the isomerization kinetics of diastereomers for $[Ln(DTPA\text{-}bz\text{-}NH_2)(H_2O)]^{2-}$ and $Ln(EPTPA\text{-}bz\text{-}NH_2)(H_2O)]^{2-}$; (ii) to determine the individual parameters influencing relaxivity, in particular water exchange rate, for both $[Gd(DTPA\text{-}bz\text{-}NH_2)(H_2O)]^{2-}$ diastereomers. To this end, the diastereomers of the lanthanide complexes have been separated by HPLC and their reconversion studied as a function of the pH. On the individual diastereomers of $[Gd(DTPA\text{-}bz\text{-}NH_2)(H_2O)]^{2-}$ separated by HPLC we have measured variable-temperature transverse and longitudinal $^{17}O$ relaxation rates and chemical shifts, multiple field water proton relaxivities, and EPR spectra.

## Experimental Section

**Materials.** $H_5DTPA\text{-}bz\text{-}NH_2$ was purchased from Macrocyclics and used without further purification. $H_5EPTPA\text{-}bz\text{-}NH_2$ (**3**) was synthesized according to Scheme 1. Compound **1**[10] (5.59 g, 6.79 mmol) was dissolved under argon atmosphere in MeOH (120 mL). Pd/C (10%; 0.285 g) was added, and the mixture was cooled to 0 °C. $H_2$ gas was bubbled into the solution for 24 h. The mixture

(4) Meares, C. F. M.; Wensel, T. G. *Acc. Chem. Res.* **1984**, *17*, 202.
(5) Konda, S. D.; Aref, M; Brechbiel, M.; Wiener, E. C. *Invest. Radiol.* **2000**, *35*, 50.
(6) Cummins, C. H.; Rutter, E. W.; Fordyce, W. A., Jr. *Bioconjugate Chem.* **1991**, *2*, 180.
(7) Schmitt-Willich, H.; Brehm, M.; Ewers, Ch. L J.; Michl, G.; Müller-Fahrnow, A.; Petrov, O.; Platzek, J.; Radüchel, B.; Sülzle, D. *Inorg. Chem.* **1999**, *38*, 1134.
(8) Burai, L.; Tóth, É.; Merbach, A. E. *Chem. Commun*. **2003**, 2680.
(9) Laus, S.; Ruloff, R.; Tóth, É.; Merbach, A. E. *Chem.—Eur. J.* **2003**, *9*, 3555.
(10) Corson, D. T.; Meares, C. F. *Bioconjugate Chem*. **2001**, *11*, 292.

**Scheme 1.** Synthesis of $H_5$EPTPA-bz-$NH_2$ (**3**)

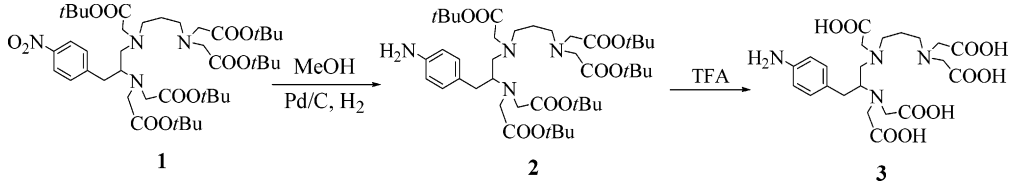


was then stirred for 2 h at room temperature. Celite was added, and the mixture was filtered through a pad of Celite to remove the catalyst. The filtrate was evaporated to dryness, and the resulting yellow oil **2** (4.98 g, 92%) was used without further purification. $^1$H NMR ($CDCl_3$, 400 MHz): $\delta$ = 1.41 (s, 9H), 1.44 (s, 18H), 1.45 (s, 18H), 1.52 (m, 2H), 2.28−2.50 (m, 8H), 3.03 (m, 1H), 3.28 (s, 2H), 3.37 (s, 4H), 3.43 (s br, 4H), 6.57 (d, 2H, $J$ = 7.8 Hz), 6.98 (d, 2H, $J$ = 7.8 Hz). MS (ESI): $m/z$ 793.3, $[M + H]^+$.

Compound **2** (4.8 g, 6.05 mmol) was dissolved in TFA (65 mL) and stirred at room temperature for 24 h. The solvent was then evaporated to dryness, and the resulting crusty yellow powder **3** (5.86 g, 99%) was obtained without further purification and stored at −18 °C. $^1$H NMR ($D_2O$, 400 MHz): $\delta$ = 2.20 (m, 2H), 2.74 (dd, $J$ = 8 Hz, $J$ = 13.8 Hz, 1H), 3.08 (dd, $J$ = 13.6 Hz, $J$ = 6.8 Hz, 1H), 3.30−3.57 (m, 11H), 4.07 (s, 1H), 4.13 (s, 1H), 4.18 (s, 4H), 7.36 (d, $J$ = 8.4 Hz, 2H), 7.42 (d, $J$ = 8.4 Hz, 2H). MS (ESI): $m/z$ 513.2, $[M + H]^+$.

All other reagents used were obtained from commercial sources. $Ln(ClO_4)_3$ stock solutions were prepared by dissolving $Ln_2O_3$ under reflux in a slight excess of $HClO_4$ (Merck, pa, 70%) in double-distilled water, followed by filtration. The concentration of $Ln(ClO_4)_3$ solutions was determined by titration with a $Na_2H_2EDTA$ solution using xylenol orange as indicator and urotropin for pH regulation. For the preparation of the LnL complexes, weighed quantities of solid ligands were dissolved in buffer solution (PIPES or TRIS, 0.01−0.1 M), and then a weighed amount of $Ln(ClO_4)_3$ stock solution was added dropwise to form the chelate complexes. The pH of the solutions was adjusted with 1 M NaOH, $HClO_4$, or HCl solutions, and the pH was measured with a combined glass electrode (C14/02-SC, Moeller Scientific Glass Instruments, Effretikon, Switzerland) connected to a Metrohm 692 pH/ion-meter calibrated with Metrohm buffer solutions.

**HPLC Methods.** All HPLC experiments were performed on a Waters 600 instrument equipped with a Waters 2487 dual-wavelength UV−vis detector and a Waters Fraction Collector II. The detection wavelengths were 240 and 290 nm.

**Method 1.** The diastereomer ratios for [Ln(DTPA-bz-$NH_2$)-($H_2O$)]$^{2-}$ complexes were determined on Waters XTerra $RP_{18}$ (5 $\mu$m, 4.6 × 150 mm) column using buffered aqueous eluent (10 mM TRIS, pH = 8, 3% acetonitrile) with 0.5 mL/min flow rate.

**Method 2.** In the study of the isomerization kinetics of [Gd-(DTPA-bz-$NH_2$)($H_2O$)]$^{2-}$, a YMC Hydrosphere $C_{18}$ column (5 $\mu$m, 4.6 × 150 mm) was used. The eluent was water containing 10 mM PIPES buffer (pH 8) and 5% acetonitrile with 0.5 mL/min flow rate. The 10 $\mu$L portions of 4 mM [Gd(DTPA-bz-$NH_2$)($H_2O$)]$^{2-}$ solution were separated collecting two fractions of pure isomers **A** and **B** (2 mL each). Five samples of each isomer (**A** and **B)** were prepared by setting the pH to 7.86, 7.27, 6.68, 6.11, and 5.60 and kept at 25 °C. The 25 $\mu$L portions of the samples were injected after given periods of time, and the quantity of the two isomers was determined.

The isomerization kinetics of [Gd(EPTPA-bz-$NH_2$)($H_2O$)]$^{2-}$ was established by modifying method 1 (2% acetonitrile and 1.0 mL/min flow rate). The 10 $\mu$L portions of the 8.7 mM solution were separated at different pHs (7.49, 7.61, 7.71, 7.91, and 8.91; TRIS buffer). The collected fractions of the minor species were kept at 25 °C, and 25 $\mu$L of those was reinjected at appropriate time intervals.

**Method 3.** A semipreparative HPLC method was developed for the separation of [Gd(DTPA-bz-$NH_2$)($H_2O$)]$^{2-}$ isomers to be used in the $^{17}$O NMR and $^1$H NMRD measurements. A 600 $\mu$L volume of 0.027 M [Gd(DTPA-bz-$NH_2$)($H_2O$)]$^{2-}$ solution was injected in 5 portions to the Waters XTerra Prep $RP_{18}$ column (10 $\mu$m, 19 × 150 mm). The eluent was 0.04 M $NH_4HCO_3$ with 10 mL/min flow rate. Two fractions for the isomers **A** and **B** were collected (approximately 150 mL). The eluates were concentrated to 20 mL by evaporation (35 °C, 30 mbar), and then 40 mL of methanol was added and evaporated to dryness. This was repeated twice with 20 mL methanol to completely remove $NH_4HCO_3$. The final products were redissolved in 300 $\mu$L of 0.1 M TRIS buffer and used for the $^{17}$O NMR and $^1$H NMRD experiments. The purity of the isomers was checked by method 1 and found to be 98.8% and 98.9% for **A** and **B**, respectively. The concentration of the samples was determined from the peak area of **A** and **B** using the [Gd(DTPA-bz-$NH_2$)($H_2O$)]$^{2-}$ calibration series. In certain cases, the $Gd^{III}$ concentration of the samples was also verified by ICP measurements.

**$^{17}$O NMR Measurements.** For the variable-temperature studies, the [Gd(DTPA-bz-$NH_2$)($H_2O$)]$^{2-}$ solutions were filled with a syringe into glass spheres which were fitted into 10 mm NMR tubes. Glass spheres are used to eliminate susceptibility effects on the chemical shift.[11] The $1/T_1$ and $1/T_2$ relaxation rates and chemical shifts were measured with regard to a 0.1 M TRIS aqueous solution (pH = 9.0) as external reference. To improve sensitivity, $^{17}$O-enriched water (10% $H_2{}^{17}O$, Yeda (Israel)) was added to the solutions to yield in 1−2% $^{17}$O enrichment. The $^{17}$O NMR measurements were performed on a Bruker ARX-400 spectrometer at 9.4 T and 54.2 MHz. Bulk water longitudinal relaxation rates, $1/T_1$, were obtained by the inversion recovery method,[12] and transverse relaxation rates, $1/T_2$, by the Carr−Purcell−Meiboom−Gill spin−echo technique.[13] The least-squares fit of $^{17}$O NMR data was performed with the program Scientist for Windows by Micromath, version 2.0. The reported errors correspond to one standard deviation obtained by the statistical analysis.

**$^1$H NMRD Measurements.** The $1/T_1$ nuclear magnetic relaxation dispersion (NMRD) profiles of the solvent protons at 25 °C were obtained on a Spinmaster FFC fast field cycling NMR relaxometer (Stelar), covering a continuum of magnetic fields from 2.35 × $10^{-4}$ to 0.47 T (corresponding to a proton Larmor frequency range 0.02−20 MHz). Higher frequency measurements were performed on a 50, 100, and 200 MHz magnet, connected to an Avance-200 console, and at 400 MHz on a Bruker ARX-400 spectrometer.

**EPR.** EPR spectra have been recorded at Q-band (35 GHz; at ambient temperature) on Elexsys E500 and at W-band (95 GHz; $T$ = 286 K) on Elexsys E680 Bruker spectrometers.

(11) Hugi, A. D.; Helm, L.; Merbach, A. E. *Helv. Chim. Acta* **1985**, *68*, 508.
(12) Vold, R. V.; Waugh, J. S.; Klein, M. P.; Phelps, D. E. *J. Chem. Phys.* **1968**, *48*, 3831.
(13) Meiboom, S.; Gill, D. *Rev. Sci. Instrum.* **1958**, *29*, 688.

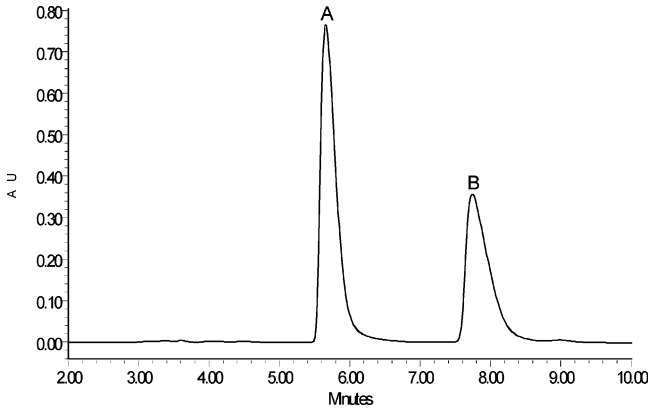


**Figure 1.** HPLC separation of $[Gd(DTPA\text{-}bz\text{-}NH_2)(H_2O)]^{2-}$ diastereomers.

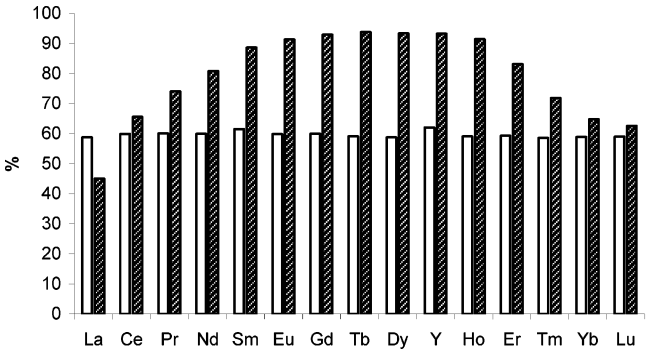


**Figure 2.** Percentage of the major (**A**) isomer of $[Ln(DTPA\text{-}bz\text{-}NH_2)(H_2O)]^{2-}$ (white column) and $[Ln(EPTPA\text{-}bz\text{-}NH_2)(H_2O)]^{2-}$ (dark column) complexes.

## Results and Discussion

The two diastereomeric forms, **A** and **B**, of $[Ln(DTPA\text{-}bz\text{-}NH_2)(H_2O)]^{2-}$ complexes were separated by HPLC for the whole series of lanthanides (following the notation introduced by Schmitt-Willich et al. for $[Gd(S\text{-}EOB\text{-}DTPA)(H_2O)]^{2-}$,[7] we call the two components **A** and **B** according to the order of elution). For each lanthanide complex, one major (**A**) and one minor peak (**B**) appear in the chromatogram with retention times ranging between 5.54 and 6.01 min and 7.47−8.44 min, for **A** and **B**, respectively (Figure 1). The ratio of the two isomers has been determined from the peak areas and found to be practically constant (around 60:40 for **A**:**B**; see Supporting Information Table S1) along the lanthanide series. The ratio of 62:38 obtained by us for $[Y(DTPA\text{-}bz\text{-}NH_2)(H_2O)]^{2-}$ is in good agreement with the 60:40 ratio published by Cummins et al.[6] Similar and metal-independent ratios were reported for EOB-DTPA complexes (65:35, 60:40, and 57:43 for Gd, La, and Eu complexes, respectively).[7,14]

The lanthanide-independent diastereomeric ratios for the $[Ln(DTPA\text{-}bz\text{-}NH_2)(H_2O)]^{2-}$ and other DTPA-derivative complexes contrast strikingly with those communicated for $[Ln(EPTPA\text{-}bz\text{-}NH_2)(H_2O)]^{2-}$ and $[Ln(EPTPA\text{-}bz\text{-}NO_2)(H_2O)]^{2-}$, where there is a large variation in the ratio along the lanthanide series.[8] In comparison to DTPA,$^{5-}$ the ligand $EPTPA^{5-}$ possesses one additional $CH_2$ group in the amine backbone. Figure 2 compares the percentage of the major (**A**) isomer for $[Ln(DTPA\text{-}bz\text{-}NH_2)(H_2O)]^{2-}$ and $[Ln(EPTPA\text{-}bz\text{-}NH_2)(H_2O)]^{2-}$ complexes. In the case of $[Ln(EPTPA\text{-}bz\text{-}NH_2)(H_2O)]^{2-}$, the fraction of the **A** isomer shows a maximum in the middle of the Ln series. Noteworthy, on mixing of buffered EPTPA and lanthanide solutions, the initial diastereomer ratio is around 50:50 for any lanthanide. Afterward, a slow interconversion of **B** to **A** occurs until the equilibrium values as indicated in Figure 2 are reached. The explanation of this phenomenon is still an open question. In contrast, such interconversion following the complex formation is not observed for DTPA complexes; the **A:B** ratio measured immediately after mixing the ligand and the metal remains constant even after several months.

In the analysis of all chromatograms, as recorded by UV−vis detection, we assume that the two diastereomers have identical molar absorption coefficients.[7] This was previously proved for the $Eu(EPTPA\text{-}bz\text{-}NH_2)^{2-}$ diastereomers: here the transformation of **B** to **A** was also monitored by recording $^1H$ NMR spectra as a function of time following the mixing of the ligand with $Eu^{3+}$.[8] In parallel, HPLC injections were done after the same periods of time. In the NMR spectrum two series of signals appear that we assign to the two diastereomers. At any time point, the integral of their NMR peaks corresponds to the integral of the HPLC peaks. On the other hand, the **A**:**B** ratio of $[Eu(DTPA\text{-}bz\text{-}NH_2)(H_2O)]^{2-}$ determined from $^1H$ NMR does not change with temperature (<1% between 0 and 50 °C) or pH ($5 < pH < 9$).

It has also to be noted that the assignment of the chromatographic peaks to the corresponding diastereomeric structure is still not clarified. The commercially available $DTPA\text{-}bz\text{-}NH_2$ ligand is in a racemic form (4*R* and 4*S*); thus, the two chromatographic peaks in Figure 1 represent most likely the coelution of 4*S*6*S*/4*R*6*R* and 4*S*6*R*/4*R*6*S* diastereomers. A $^1H$ and $^{13}C$ NMR study has been performed on the diamagnetic $La^{3+}$ complex of the optically pure *S*-EOB-DTPA.[7] It was concluded that the two isomers differ in the configuration of the central nitrogen (6th position). Most presumably, the major isomer (**A**) has 4*S*6*R*, whereas the minor (**B**) isomer has 4*S*6*S* configuration. Additional NMR and chiroptical experiments on $[Eu(S\text{-}EOB\text{-}DTPA)(H_2O)]^{2-}$ support this assumption and prove the Λ helicity around the metal center.[14]

**Isomerization Rate.** In the preliminary communication on $[Gd(EPTPA\text{-}bz\text{-}NH_2)(H_2O)]^{2-}$ and $[Gd(EPTPA\text{-}bz\text{-}NO_2)(H_2O)]^{2-}$, we reported the relaxation properties of the two individual isomers; however, detailed kinetic measurements regarding the interconversion of the isomers were not performed.[8] We qualitatively observed that the rate of interconversion was relatively fast, and this prevented us from measuring the properties of **A** and **B** in HPLC-separated samples containing exclusively one isomer.

In contrast to EPTPA, isomer transformation was found to be slow for EOB-DTPA complexes.[7] A variable-pH and -temperature kinetic study on $[Gd(EOB\text{-}DTPA)(H_2O)]^{2-}$ showed that the transformation is a slow, acid-catalyzed process, with $t_{1/2} = 150.9$ h at pH 7.0 and 25 °C.[7]

(14) Thompson, N. C.; Parker, D.; Schmitt-Willich, H.; Sülzle, D.; Muller, G.; Riehl, J. P. *J. Chem. Soc., Dalton Trans.* **2004**, 1892.

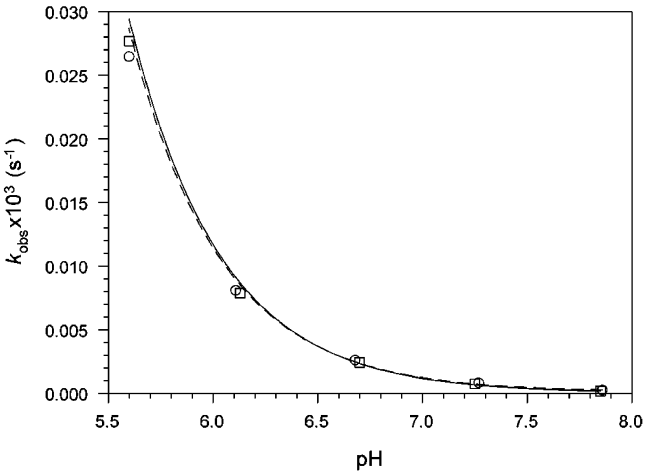


**Figure 3.** $k_{obs}$ rate constants as a function of pH for the isomerization of [Gd(DTPA-bz-NH$_2$)(H$_2$O)]$^{2-}$ diastereomers and the result of the fit. Squares and the solid line represent the reaction from **A** to **B**, and circles and the dashed line, the reaction from **B** to **A**.

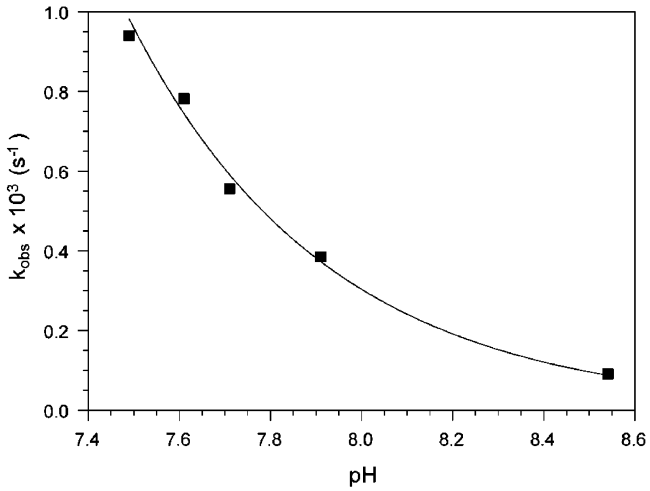


**Figure 4.** $k_{obs}$ rate constants as a function of pH for the isomerization of [Gd(EPTPA-bz-NH$_2$)(H$_2$O)]$^{2-}$ diastereomers.

We have studied the isomerization kinetics of [Gd(DTPA-bz-NH$_2$)(H$_2$O)]$^{2-}$ diastereomers at variable pH. A concentrated stock solution of the complex was separated on an analytical column to obtain samples containing >99% pure **A** and **B** isomers (HPLC method 2; see Experimental Section). After the appropriate pH was set, the transformation of the isomers occurring in a thermostated solution (25 °C) was monitored in time by using HPLC method 2. The isomerization of both **A** and **B** correspond to a first-order kinetic reaction.

$$\mathbf{A} \underset{k_{AB}}{\overset{k_{BA}}{\rightleftharpoons}} \mathbf{B} \qquad (1)$$

The kinetic data obtained, i.e., the *A* and *B* molar fractions at times *t*, were fitted to a single-exponential curve as follows. from **A** to **B**:

$$A = (A_0 - A_f)e^{-k_{AB}t} + A_f \qquad (2)$$

from **B** to **A**:

$$B = (B_0 - B_f)e^{-k_{BA}t} + B_f \qquad (3)$$

Here $A_0$ and $B_0$ are the initial, whereas $A_f$ and $B_f$ are the final (equilibrium), molar fractions of **A** and **B** isomers in the solution. The observed rate constants, $k_{AB}$ and $k_{BA}$ (hereafter $k_{obs}$), are identical within the experimental error at any pH. The experimental $k_{obs}$ values are presented in Figure 3 as a function of pH. According to proton catalysis, $k_{obs}$ increases with decreasing pH and is linearly proportional to the $H^+$ concentration:

$$k_{obs} = k_0 + k_1[H^+] \qquad (4)$$

When the experimental $k_{obs}$ values were fitted, $k_1 = 11.7 \pm 0.5$ and $11.4 \pm 0.7$ s$^{-1}$ M$^{-1}$ second-order rate constants were calculated for the transformation from **A** to **B** and from **B** to **A**, respectively. The $k_1$ value for [Gd(DTPA-bz-NH$_2$)(H$_2$O)]$^{2-}$ is three times higher than that of obtained for [Gd(EOB-DTPA)(H$_2$O)]$^{2-}$, 3.92 s$^{-1}$ M$^{-1}$.[7] As the transformation of the diastereomers occurs via the breaking and re-formation of the coordination bond between the metal and the donor atoms, the pending arm on the ligand has only limited influence on the interconversion rate. The faster isomerization of [Gd(DTPA-bz-NH$_2$)(H$_2$O)]$^{2-}$ may be the consequence of the amino group on the benzyl arm which can protonate and assist the acid catalysis. (The protonation constant has not been determined for this amine group; however, it is known for aniline, log $K = 4.7$). Presumably, a spontaneous isomerization pathway without participation of protons, described by the $k_0$ rate constant, cannot be excluded either. Dissociation and metal exchange kinetic studies on [Ln(DTPA)(H$_2$O)]$^{2-}$ derivatives showed that spontaneous dissociation also occurs in addition to the proton-catalyzed process.[15] However, the $k_0$ rate constant was obtained with a large error; thus, at least in this pH range, no reliable value of $k_0$ can be calculated. Most likely $k_0$ is on the order of $10^{-8}$–$10^{-9}$ s$^{-1}$.

For a direct comparison, the isomerization rate of [Gd(EPTPA-bz-NH$_2$)(H$_2$O)]$^{2-}$ diastereomers has also been measured. Only the transformation of the minor isomer of [Gd(EPTPA-bz-NH$_2$)(H$_2$O)]$^{2-}$ was monitored after separation. The pH range of these experiments was higher than that of used for [Gd(DTPA-bz-NH$_2$)(H$_2$O)]$^{2-}$, as below pH 7.5 the transformation of the [Gd(EPTPA-bz-NH$_2$)(H$_2$O)]$^{2-}$ diastereomers is too fast to be followed by HPLC. The $k_{obs}$ rate constants measured are presented in Figure 4. The $k_1$ second-order rate constant calculated is $(3.03 \pm 0.07) \times 10^4$ s$^{-1}$ M$^{-1}$, around 2500 times higher than that for [Gd(DTPA-bz-NH$_2$)(H$_2$O)]$^{2-}$. The faster isomerization of [Gd(EPTPA-bz-NH$_2$)(H$_2$O)]$^{2-}$ can be most likely explained in terms of a faster dissociation of the complex to form free ligand and metal as compared to [Gd(DTPA-bz-NH$_2$)(H$_2$O)]$^{2-}$. Although a detailed kinetic study of the dissociation and metal exchange reaction of [Gd(EPTPA)(H$_2$O)]$^{2-}$ is not yet available, it is very plausible that, due to its elongated amine backbone, this complex is kinetically less inert than

(15) (a) Brücher, E.; Laurenczy, G. *J. Nucl. Chem.* **1981**, *41*, 2089. (b) Sarka, L.; Burai, L.; Brücher, E. *Chem.—Eur. J.* **2000**, *6*, 719. (c) Burai, L.; Brücher, E.; Király, R.; Solymosi, P.; Víg, T. *Acta Pharm. Hung.* **2000**, *70*, 89.

$[Gd(DTPA)(H_2O)]^{2-}$. In conclusion, $[Ln(DTPA\text{-}bz\text{-}NH_2)(H_2O)]^{2-}$ diastereomers transform slowly enough to maintain sufficient isomer purity over a long period after separation. Hence, $[Ln(DTPA\text{-}bz\text{-}NH_2)(H_2O)]^{2-}$ and other DTPA derivatives are appropriate for diverse investigations of the individual diastereomers.

**Water Exchange Rate.** For Gd-chelate complexes used as MRI contrast agents it is a basic requirement to have at least one water molecule in the inner coordination sphere. The inner sphere water molecule is in exchange with the bulk so that the paramagnetic relaxation enhancement effect of $Gd^{3+}$ is transferred to the environment. The rate of water exchange from the inner sphere to the bulk can be directly determined by variable-temperature $^{17}O$ NMR relaxation measurements.

Despite the relatively fast isomerization of $[Gd(EPTPA\text{-}bz\text{-}NH_2)(H_2O)]^{2-}$, the individual water exchange rate of the two isomers could be measured by taking advantage of their approximately equal ratio on complex formation and their subsequent transformation to the equilibrium state (93:7 **A:B**), as reported previously.[8] Concomitant to the transformation of **B** to **A**, the $1/T_2$ relaxation rates increase with time for both $[Gd(EPTPA\text{-}bz\text{-}NH_2)(H_2O)]^{2-}$ and $[Gd(EPTPA\text{-}bz\text{-}NO_2)(H_2O)]^{2-}$ complexes showing that the two diastereomers have different water exchange rates. The evolution of the $^{17}O$ $1/T_2$ relaxation rates was monitored after mixing buffered $Gd^{3+}$ and EPTPA-bz-$NH_2$ or EPTPA-bz-$NO_2$ solutions, and parallel HPLC injections from the same samples were done to measure the diastereomer ratio in the given time period. From the variation of the $1/T_2$ values over time and by using the **A:B** ratios determined by HPLC for each time point, the water exchange rates were calculated. We assumed that the electronic relaxation parameters and the hyperfine coupling constant were identical for the two isomers, and we used the values previously determined for $[Gd(EPTPA\text{-}bz\text{-}NO_2)(H_2O)]^{2-}$ (equilibrium mixture of **A** and **B**).[9] Although not spectacular, the difference in the water exchange rate was well distinct between the two $[Gd(EPTPA\text{-}bz\text{-}NH_2)(H_2O)]^{2-}$ and $[Gd(EPTPA\text{-}bz\text{-}NO_2)(H_2O)]^{2-}$ isomers. In both cases, the $k_{ex}$ values roughly doubled from the **A** (93%) to the **B** (7%) isomer ($k_{exi}^{298}$ is $(1.4 \pm 0.1) \times 10^8$ and $(2.6 \pm 0.2) \times 10^8$ $s^{-1}$ for **A** and **B** of $[Gd(EPTPA\text{-}bz\text{-}NO_2)(H_2O)]^{2-}$ and $(1.8 \pm 0.1) \times 10^8$ and $(4.4 \pm 0.2) \times 10^8$ $s^{-1}$ for **A** and **B** of $[Gd(EPTPA\text{-}bz\text{-}NH_2)(H_2O)]^{2-}$). This implies that, e.g. for $[Gd(EPTPA\text{-}bz\text{-}NH_2)(H_2O)]^{2-}$, the **B** isomer, present in 7%, is responsible for 16% of the overall water exchange.

In contrast to the EPTPA-derivative complexes, for $[Gd(DTPA\text{-}bz\text{-}NH_2)(H_2O)]^{2-}$ the water exchange rate could be measured on the separated, pure diastereomers. After HPLC separation, their isomerization rate is slow enough to maintain the isomer purity for the time of the entire $^{17}O$ NMR experiment even at higher temperatures; thus, the classical technique was used for water exchange rate determination. We had three samples containing (1) the pure major isomer (**A**), (2) the pure minor isomer (**B**), and (3) a nonseparated $[Gd(DTPA\text{-}bz\text{-}NH_2)(H_2O)]^{2-}$ solution in isomer equilibrium state (**AB**; 60% **A** and 40% **B**). The oxygen-17 $1/T_1$, $1/T_2$ relaxation rates and chemical shift of the samples were measured in the temperature range 0−70 °C referred to a buffered aqueous sample at identical pH. At the end of the experiments, the isomer purity of solutions **A** and **B** was checked and found >99%. The results of the $^{17}O$ NMR experiments are presented in Figure 5.

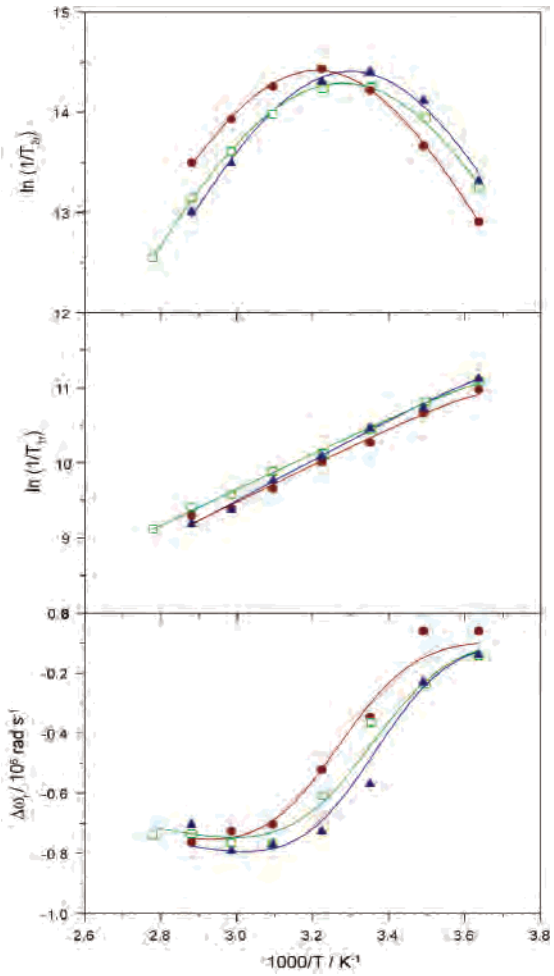


**Figure 5.** Reduced transverse (top) and longitudinal (middle) $^{17}O$ relaxation rates and reduced $^{17}O$ chemical shifts (bottom) as a function of the inverse temperature measured in separated samples of **A** (red circles) and **B** (blue triangles) diastereomers of $[Gd(DTPA\text{-}bz\text{-}NH_2)(H_2O)]^{2-}$ and in an equilibrium mixture of **A** and **B** (green squares). The lines correspond to the fitted curves using the Solomon−Bloembergen−Morgan theory of paramagnetic relaxation. The reduced transverse ($1/T_{2r}$) and longitudinal relaxation rates ($1/T_{1r}$) and chemical shifts ($\Delta\omega_r$) are defined as follows, where $T_{1,2}$ and $\omega$ are the longitudinal and transverse relaxation rates and chemical shifts measured in the $Gd^{III}$ complex solution, whereas $T_{1,2A}$ and $\omega_A$ are those measured in a diamagnetic reference solution and $P_m$ is the molar fraction of coordinated water: $1/T_{1,2r} = (1/P_m)[1/T_{1,2} - 1/T_{1,2A}]$; $\Delta\omega_r = (1/P_m)(\omega - \omega_A)$.

The reduced transverse $^{17}O$ relaxation rates, $1/T_{2r}$, are in all three cases in the fast exchange region at higher and in the slow exchange region at lower temperatures with a changeover around 300 K for **B** and 320 K for **A**, the **AB** sample being in between. The reduced chemical shifts at higher temperatures are very similar for the three samples showing that both diastereomers have the same number of inner sphere water molecule ($q$). For analogous $[Gd(DTPA)(H_2O)]^{2-}$ derivatives one inner sphere water molecule was reported; thus, we assume $q = 1$ for $[Gd(DTPA\text{-}bz\text{-}NH_2)$-

**Table 1.** Parameters Characterizing Water Exchange, Rotation, and Electron Spin Relaxation As Obtained from $^{17}$O NMR Data for **A** and **B** Diastereomers of [Gd(DTPA-bz-NH$_2$)(H$_2$O)]$^{2-}$ and for the Equilibrium Solution **AB** (60% **A** and 40% **B**)[a,b]

| | A | B | AB | [Gd(DTPA)-(H$_2$O)]$^{2-}$ [c] |
|---|---|---|---|---|
| $k_{ex}^{298}/10^6$ s$^{-1}$ | 5.7 ± 0.2 | 3.1 ± 0.1 | 4.7 ± 0.1 | 4.1 |
| $\Delta H^{\ddagger}$/kJ mol$^{-1}$ | 54.4 ± 1.1 | 53.5 ± 1.1 | 51.9 ± 0.7 | 52.0 |
| $\Delta S^{\ddagger}$/J mol$^{-1}$ K$^{-1}$ | +66.8 ± 3.4 | +58.6 ± 3.7 | +57.0 ± 3.2 | +56.2 |
| $(A/\hbar)/10^6$ rad s$^{-1}$ | −3.7 ± 0.1 | −3.6 ± 0.1 | −3.5 ± 0.1 | −3.8 |
| $\tau_R^{298}$/ps | 246 ± 5 | 223 ± 5 | 256 ± 4 | 103 |
| $E_R$/kJ mol$^{-1}$ | 22.3 ± 0.7 | 20.4 ± 0.7 | 19.7 ± 0.4 | 18 |
| $\tau_v^{298}$/ps | 19 ± 2 | 20 ± 2 | 21 ± 1 | 0.25 |
| $E_v$/kJ mol$^{-1}$ | 1 | 1 | 1 | 1.6 |
| $\Delta^2/10^{20}$ s$^{-2}$ | 2.5 ± 0.2 | 2.4 ± 0.2 | 3.0 ± 0.2 | 0.15 |
| $C_{os}$ | 0.1 | 0.1 | 0.1 | 0.2 |

[a] Italicized values were fixed in the fit. [b] The equations used in the analysis of the $^{17}$O NMR data are listed in the Supporting Information. The following parameters are calculated: $k_{ex}^{298}$, water exchange rate at 298 K; $\Delta H^{\ddagger}$, activation enthalpy of water exchange; $\Delta S^{\ddagger}$, activation entropy of water exchange; $A/\hbar$, hyperfine coupling constant, between the water oxygen and Gd$^{3+}$; $\tau_R^{298}$, rotational correlation time of the complex at 298 K; $E_R$, activation energy of rotation; $\tau_v^{298}$, electronic zero-field-splitting modulation time at 298 K; $E_v$, activation energy of electronic zero-field-splitting; $\Delta^2$, trace of the square of the transient zero-field-splitting tensor; $C_{os}$, outer-sphere contribution to the chemical shift. [c] Reference 16.

(H$_2$O)]$^{2-}$.This is confirmed by the values of the hyperfine coupling constant, $A/\hbar$, obtained from the analysis of the chemical shift data (see below). The experimental data have been fit to the Solomon−Bloembergen−Morgan theory which was successfully applied for many Gd−poly(amino carboxylate) complexes.[16] The parameters describing water exchange, rotation, and electronic relaxation, as obtained from the fit, are compared in Table 1 for **A**, **B**, and **AB** samples and for [Gd(DTPA)(H$_2$O)]$^{2-}$.

The water exchange is faster, though not dramatically, for the **A** than for the **B** isomer of [Gd(DTPA-bz-NH$_2$)(H$_2$O)]$^{2-}$ ($k_{ex}^{298}$ is 5.7 × 10$^6$ and 3.1 × 10$^6$ s$^{-1}$ for **A** and **B**, respectively). In the equilibrium solution (**AB**) with 60% **A** and 40% **B**, the water exchange rate measured, $k_{ex}^{298} = 4.7 \times 10^6$ s$^{-1}$, agrees well with that calculated from values for **A** and **B**, 4.66 × 10$^6$ s$^{-1}$. Interestingly, the ratio of $k_{ex}^{298}$ for **A** and **B** is close to 2, similar to that found for the diastereomers of Gd(EPTPA)$^{2-}$ derivatives. However, on the basis of only two examples, it is difficult to state any general rule in this respect. In comparison to other [Gd(DTPA)-(H$_2$O)]$^{2-}$ derivatives, [Gd(DTPA-bz-NH$_2$)(H$_2$O)]$^{2-}$ has a similar water exchange rate ($k_{ex}^{298} = 4.1 \times 10^6$ and 3.6 × 10$^6$ s$^{-1}$ for [Gd(DTPA)(H$_2$O)]$^{2-}$ and [Gd(EOB-DTPA)-(H$_2$O)]$^{2-}$, respectively).[16,17] This let us conclude that the aminobenzyl pending arm on the DTPA has only minor influence on the water exchange.

For the macrocyclic LnDOTA$^-$ complexes, often paralleled with the acyclic DTPA family, the existence of diastereomers is a well-described phenomenon. It is the consequence of the different orientation of the acetate groups and the different dihedral angles of the ethylene bridges in the tetraazacyclododecane ring. Basically, the two diastereomers display a different orientation of the two square planes formed by the four cyclen nitrogens and the four binding oxygens, making an angle of ca. 40° in one of the structures (**M**-type) whereas it is reversed and reduced to ca. 20° in the **m**-type structures. In solution, the two isomers, **m** and **M**, may exist in equilibrium.[18] In solid state for [Ln(DOTA)(H$_2$O)]$^{3+}$ complexes, **m**-type structures have been observed for La and Ce and **M**-type structures for Eu, Gd, Dy, Ho, Lu, and Y.[19] These diastereomers cannot be separated by HPLC techniques as they interchange very quickly (for the **m** → **M** process a rate of $k = 511$ s$^{-1}$ was reported at 306 K).[18] However, they are well distinguishable by $^1$H or $^{13}$C NMR spectroscopy. The water exchange rate has been directly assessed on the two diastereomers of the tetraamide derivative [Eu(DOTAM)(H$_2$O)]$^{3+}$ in acetonitrile−water solvent.[20] The water exchange on **m** is about 50 times faster than on **M**, and even though the equilibrium constant $K = [\mathbf{M}]/[\mathbf{m}]$ equals 4.5, the contribution of **m** to the overall exchange rate represents 90%.

The difference observed in the water exchange rate of the diastereomers of the linear DTPA− or EPTPA−Gd$^{III}$ complexes is of no weight compared to this enormous variation for the macrocyclic complexes. It is clear that in the two cases the origin of the presence of diastereomers is fundamentally different. Clearly, the structural difference between the **m** and **M** isomers for DOTA-type complexes acts much more upon the inner coordination sphere and consequently modifies more strongly the water exchange rate than for the linear chelates. In this latter case, the differing configuration of the carbon in position-4 or that of the central nitrogen in the ligand will not essentially influence the inner coordination sphere of the complex, which could in turn lead to significantly different water exchange rates.

When the $^{17}$O NMR data are fitted to the Solomon−Bloembergen−Morgan theory, the parameters describing electron spin relaxation are also calculated. The recent development in the field of electronic relaxation of Gd$^{III}$ complexes showed that this model is not really adequate; however, due to its relative simplicity, it remains widely used.[21] Therefore, we do not wish to interpret in details the parameters obtained in our fit. Nevertheless, they show that electronic relaxation does not differ basically for the two diastereomers **A** and **B** and the mixture **AB**. This is also supported by EPR measurements performed at different fields on separated samples of **A**, **B**, and the equilibrium solution

(16) Micskei, K.; Helm, L.; Brücher, E.; Merbach, A. E. *Inorg. Chem.* **1993**, *32*, 3844.
(17) Tóth, É.; Burai, L.; Brücher, E.; Merbach, A. E. *J. Chem. Soc., Dalton Trans.* **1997**, 1587.
(18) Aime, S.; Botta, M.; Fasano, M.; Marques, M. P. M.; Geraldes, C. F. G. C.; Pubanz, D.; Merbach, A. E. *Inorg. Chem.* **1997**, *36*, 259.
(19) (a) Aime, S.; Barge, A.; Botta, M.; Fasano, M.; Ayala, J. D.; Bombieri, G. *Inorg. Chim. Acta* **1996**, *246*, 423. (b) Parker, D.; Pulukkody, K.; Smith, F. C.; Batsanov, A.; Howard, J. A. K. *J. Chem. Soc., Dalton Trans.* **1994**, 689. (c) Benetollo, F.; Bombieri, G.; Aime, S.; Botta, M. *Acta Crystallogr., Sect. C: Cryst. Struct. Commun.* **1999**, *55*, 353. (d) Dubost, J. P.; Leger, J. M.; Langlois, M. H.; Meyer, D.; Schaefer, M. *C. R. Acad. Sci. Paris* **1991**, *312*, 349.
(20) (a) Aime, S.; Barge, A.; Bruce, J. I.; Botta, M.; Howard, J. A. K.; Moloney, J. M.; Parker, D.; De Sousa, A. S.; Woods, M. *J. Am. Chem. Soc.* **1999**, *121*, 5762. (b) Aime, S.; Barge, A.; Botta, M.; De Sousa, A. S.; Parker, D. *Angew. Chem., Int. Ed.* **1998**, *37*, 2673. (c) Dunand, A. F.; Aime, S.; Merbach, A. E. *J. Am. Chem. Soc.* **2000**, *122*, 1506.
(21) Borel, A.; Helm, L.; Merbach, A. E. In *Very High Frequency (VHF) ESR/EPR*; Vol. 22 of Biological Magnetic Resonance; Plenum Press: New York, 2004; pp 219−260.

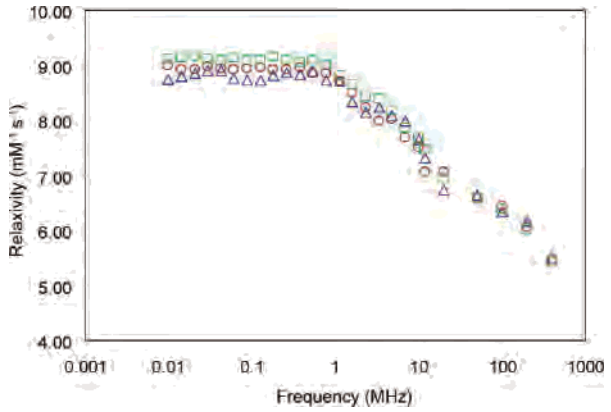


**Figure 6.** Water proton relaxivities measured in separated samples of **A** (red circles) and **B** (blue triangles) diastereomers of $[Gd(DTPA\text{-}bz\text{-}NH_2)(H_2O)]^{2-}$, as well as in an equilibrium mixture of **A** and **B** (green squares).

**AB**. For the three samples, the peak-to-peak line widths were equal within experimental error (Supporting Information). Similarly, after mixing EPTPA-$NO_2^{5-}$ or EPTPA-$NH_2^{5-}$ with $Gd^{3+}$ we detected no change in the X-band EPR peak-to peak line widths as a function of time. This means that the isomerization process, which occurs from the formation of the complex with 1:1 **A:B** ratio until equilibrium, does not affect the electronic relaxation; thus, it must be the identical for **A** and **B**.

Water proton relaxivities have been also measured for the two $[Gd(DTPA\text{-}bz\text{-}NH_2)(H_2O)]^{2-}$ diastereomers. As it is presented in Figure 6, the relaxivity profiles for **A** and **B** isomers as well as for the equilibrium state (**AB**) of $[Gd(DTPA\text{-}bz\text{-}NH_2)(H_2O)]^{2-}$ are the same within the experimental error. For the low molecular weight complexes the relaxivity is limited by rotation rather than water exchange. As a consequence, the different water exchange rate on the two diastereomers has practically no influence on the relaxivity which is determined by the fast rotation. Due to its larger size, $[Gd(DTPA\text{-}bz\text{-}NH_2)(H_2O)]^{2-}$ has a longer rotational correlation time than $[Gd(DTPA)(H_2O)]^{2-}$ ($\tau_R^{298}$ = 256 ps vs 103 ps, respectively) which is reflected in its higher relaxivity; $r_1 = 7.6\ mM^{-1}\ s^{-1}$ in comparison to 5.6 $mM^{-1}\ s^{-1}$ for $[Gd(DTPA)(H_2O)]^{2-}$ at 10 MHz and 25 °C.

## Conclusion

An HPLC analysis showed that the diastereomer ratio for $Ln^{III}$ DTPA derivatives remains constant throughout the lanthanide series, in contrast to the previously described $Ln^{III}$ EPTPA derivatives, where it varied as a function of the cation size with a maximum for the middle lanthanides. The interconversion between the two diastereomers of $[Gd(DTPA\text{-}bz\text{-}NH_2)(H_2O)]^{2-}$ is a proton-catalyzed process, which is slow enough to allow for investigating the individual isomers in pure form after HPLC separation. The water exchange rate has been determined for both isomers and, similarly to $Ln^{III}$ EPTPA derivatives, was found to differ by a factor of 2. This variance in the exchange rate has no consequence on the water proton relaxivity of the two diastereomers, since it is solely limited by fast rotation. However, such difference in $k_{ex}$ will considerably affect proton relaxivity when these diastereomers are linked to a slowly rotating macromolecule. Once the rotation is optimized, it is the slow water exchange which will exclusively or partly limit relaxivity; in this case a factor of 2 in the water exchange rate can lead to a remarkably different relaxivity for the two macromolecular diastereomer complexes. Consequently, these results have important implications for future development of $Gd^{III}$-based, macromolecular MRI contrast agents, since, due to the use of bifunctional ligands, their synthesis inevitably involves the presence of diastereomers.

**Acknowledgment.** This paper is dedicated to Professor Ernõ Brücher on the occasion of his 70th birthday. The authors are grateful to Meriem Benmelouka for the EPR measurements. This research was financially supported by the Swiss National Science Foundation and the Office for Education and Science (OFES). This work was carried out in the frame of the EC COST Action D18.

**Supporting Information Available:** Tables of the diastereomeric ratios for $[Ln(DTPA\text{-}bz\text{-}NH_2)(H_2O)]^{2-}$ and $[Ln(EPTPA\text{-}bz\text{-}NH_2)(H_2O)]^{2-}$, the experimental and calculated rate constants for the isomerization reaction, results of the variable-temperature $^{17}O$ NMR measurements, transverse electron spin relaxation rates, and the relaxivity values, as well as equations of the Solomon−Bloembergen−Morgan theory used for the analysis of $^{17}O$ NMR data. This material is available free of charge via the Internet at http://pubs.acs.org.

IC048645D